Variation of structural vibration characteristics versus non-uniform temperature distribution

Yong Xia[a,*], You-Lin Xu[a], Ze-Long Wei[a], Hong-Ping Zhu[b], and Xiao-Qing Zhou[c]

[a] *Department of Civil and Structural Engineering, The Hong Kong Polytechnic University, Hung Hom, Kowloon, Hong Kong, China*

[b] *School of Civil Engineering & Mechanics, Huazhong University of Science & Technology, Wuhan, Hubei, 430074, China*

[c] *College of Civil Engineering, Shenzhen University, Shenzhen, Guangdong, China*

Abstract

In vibration-based condition assessment exercises, it is necessary to discriminate the variation of structural properties due to environmental changes from those caused by structural damage. Some efforts have been made to correlate the structural vibration characteristics and the air temperature or temperatures at the structural surface. As the temperature of an entire structure is generally non-uniformly distributed, using the air temperature or surface temperatures alone may not sufficiently capture the relation between the structural responses and temperatures. The present paper aims to investigate the variation of the structural vibration characteristics versus the non-uniform temperature field of the structure. Thermodynamic models are employed to estimate the temperature at different components of the structure at different time. As the material mechanical properties are temperature dependent, the structure can be regarded as a composite structure consisting of elements with different Young's moduli. Consequently the natural frequencies of the structure can be calculated with the finite

[*] Corresponding author. Tel.: +852 2766 6066; fax: +852 2334 6389.
E-mail address: ceyxia@polyu.edu.hk (Dr. Yong Xia)

element method. The procedures are repeated for different time and thus variation of the frequencies with respect to time is obtained. A simply-supported RC slab was constructed and used as a proof-of-concept example. The temperatures at different points of the slab were recorded continuously in one day, together with a series of forced modal testing to extract its modal properties. On the other hand, a finite element model was established to conduct a transient thermal analysis and estimate the temperature distribution of the slab, which shows a good agreement with the measurement counterpart. The temperature data at all components and thermal properties of the material were then inputted to the model to calculate the frequencies, which also matched the measured frequencies very well. Moreover, a good linear correlation between the natural frequencies measured and the structural temperatures other than the air temperature or surface temperatures is observed. The present study provides a new approach to quantify the environmental effect on the structural vibration characteristics.

Keywords: Structural condition assessment; temperature effect; vibration characteristics; thermodynamics; linear regression

1. Introduction

In structural condition monitoring assessment [1][2][3][4], a practical difficulty exists because the structural responses vary with the changing environmental conditions, particularly the temperature. Some studies have found that the changes in structural responses due to temperature variation could be more significant than the changes due to normal structural damage [5]. If the temperature effect is not fully understood, structural condition cannot be evaluated reliably [6].

During the past 20 years, quite a few studies have been conducted to investigate the environmental effect on structural vibration properties. Askegaard and Mossing [7] studied a three-span RC footbridge and observed a 10% seasonal change in frequency over a three-year period. Researchers from Los Alamos National Laboratory [8] found that the first three natural frequencies of the Alamosa Canyon Bridge varied about 5% during a 24 hours period as the temperature of the bridge deck changed by approximately 22°C. Peeters and De Roeck [9] continuously monitored the Z24-Bridge for nearly a year and they reported that the frequencies decreased with the temperature increase. Desjardines et al. [10] studied modal data and average girder temperature collected over a six-month period in the Confederation Bridge. The first two modal frequencies identified from the Bill Emerson Memorial Bridge [11] monotonically decreased as the temperature went up in a linear way, while the mode shapes did not experience a significant change. Ni et al. [12][13] investigated the effect of

temperature and wind speed on modal parameters in the Ting Kau Bridge in Hong Kong using one-year monitoring data. Fu and DeWolf [14] found that the changes in the frequencies of a two-span composite steel-girder bridge were due to changes in the bridge bearings. Liu and DeWolf [15] found that the frequencies of a curved concrete box bridge varied by a maximum of 6% in a peak to peak temperature range of 70°F (39°C) during one year. Breccolotti et al. [16] numerically analysed the temperature effect on a bridge through thermal analysis. Macdonald and Daniell [17] investigated the variations of natural frequencies of the Second Severn Crossing cable-stayed bridge due to wind, temperature and traffic loading. Nayeri et al. [18] monitored a 17-story steel frame building and it showed a strong correlation between the frequency and air temperature while the frequency variations lagged behind the temperature variations by a few hours. A chamber experiment which was conducted by Balmes et al. [19] demonstrated that axial stresses due to different thermal expansion in members cause the frequencies to change significantly. Xia et al. [20] have conducted experiments on a continuous concrete slab for nearly two year. It was found that the frequencies had a strong negative correlation with temperature and humidity, damping ratios had a positive correlation, but no clear correlation of mode shapes with temperature and humidity change could be observed.

In summary, it has been widely observed that natural frequencies of structures decrease when temperature goes up. In addition, most of these researches focus on establishment of the correlation between the temperatures measured on the structure

surface (or in air) and the structural responses. However, the temperature distribution in a structure is generally non-uniform and time-dependent. For most of the construction materials, it is generally accepted that an increase in temperature will cause a decrease in Young's modulus and shear modulus of the materials. Therefore, the Young's modulus throughout a structure with existence of temperature gradient is not identical. Consequently the structural responses are associated with the temperature distribution of the entire structure. Using the air temperature or surface temperatures alone may not discover the realistic relation between the structural responses and temperature sufficiently.

Under this concept, the present paper aims to quantify the temperature effect on the vibration properties of a structure by investigating the temperature distribution of the structure via a thermodynamic approach. First, the thermal field distribution of the structure will be obtained through a transient heat analysis. Second, with the temperature data at different members and the thermal properties of the structural materials, the structural mechanical properties in each member are obtained. Then the dynamic properties of the whole structure can be calculated. Finally, the relation between the temperature distribution and structural dynamic properties will be established quantitatively. The temperature data measured at some critical points at different times will be employed to verify the thermodynamic models. The calculated dynamic properties can also be compared with the measurement. A laboratory tested RC slab will be used as a proof-of-concept example to demonstrate the whole

procedures.

2. Laboratory experiment

2.1. Description of the RC slab

A simply-supported RC slab was constructed for this study which measures 3200 mm long, 800 mm wide, and 120 mm thick with 100 mm overhang at each end, as shown in Fig. 1 and Fig. 2. Grade C30 concrete was selected in accordance with the design code in People's Republic of China [21]. Φ12 mm reinforcing bars at a 150 mm interval were chosen for positive reinforcement with 15 mm cover and, Φ10 mm reinforcing bars at a 200 mm interval were laid in the perpendicular direction.

Under the sunshine, the temperatures in the top surface and bottom surface of the slab are assumed uniformly distributed in two horizontal directions, which implies the temperature gradient exists along the thickness direction of the slab only. Therefore, seven thermocouples were embedded into the slab at an interval of 20 mm along the thickness direction (marked with *T*1 to *T*7 from the top to the bottom in Fig. 1) to measure the temperature distribution in the direction. To mount the thermocouples in position and measure the temperature of concrete, a plastic tube of 120 mm long was drilled with 7 holes at an interval of 20 mm in one side and another 7 holes at identical

interval in the opposite side. The tube was placed vertically in the center of the slab before pouring concrete. The seven thermocouples were then penetrated through the 7 pairs of holes of the pipe and embedded in the concrete, as illustrated in Fig. 1b. The thermocouples were located in the center of the slab in plan, as shown in Fig. 1c. To examine the temperature distribution along horizontal direction, thermocouples were embedded in one corner to compare the temperature at the corner with the temperature in the center. Due to limitation of channels, three thermocouples were installed at the corner and placed at top of the slab, middle of the slab, and bottom of the slab (T9~T11). An additional thermocouple (T8) was employed to measure the air temperature. The figure also illustrates 14 points to install accelerometers to record the vibration of the slab subject to impact from an instrumented hammer.

2.2. Procedures of the experiment

After the slab curing 28 days, modal tests were carried out. Seven accelerometers were used to measure the vibration responses of the slab under impact from an instrumented hammer. Two sets of measurement were required to extract the mode shapes at the 14 points. Modal data (frequencies, mode shapes and damping ratios) were extracted from the frequency response functions with the Global Rational Fraction Polynomial method [22], a standard modal identification technique.

The present study aims to investigate the variation the structural vibration

characteristics with respect to different temperatures. Sets of modal testing were carried out hourly from 8:00 am to 22:00 pm on 11th Feb., 2009. At the same time, structural temperatures were automatically recorded from the embedded thermocouples every 2 minutes from 6:00 am on 11th Feb. to 6:00 am on 12th Feb., 2009. Due to space limitation on campus, the slab could be exposed to sun irradiation in the morning only and shaded by buildings in the afternoon, while this limitation does not affect the analytical methods proposed in the paper.

A previous study on a slab has found that the mode shapes were not affected by the temperature changes as the temperatures along the horizontal directions are uniformly distributed [20]. Consequently only frequencies and damping ratios were extracted from four accelerometers while the mode shapes haven't been measured during the day.

3. Temperature data

3.1. Variation of temperature in one day

The uniformly distributed 7 thermocouples captured the temperature along the thickness of the slab. Fig. 2 shows the variations of the structural temperatures in 24 hours, together with the air temperature. It shows that temperature at the slab ($T1$ to $T7$)

increased from 9:00 am to 13:30 pm and decreased after that. The temperatures near the top surface arose more significantly than the temperatures near the bottom surface, as expected. As solar irradiation was blocked by the adjacent buildings, the temperatures at *T1* and *T2* dropped down very fast in the afternoon while others decreased slower, due to the property of thermal inertia. Fig. 3 compares the temperatures measured at the center of the slab (T1, T4 and T7) with those measured at the corner (T9~T11). It is noted that T1 and T9 are the temperatures at the top, T4 and T10 are those in the middle, and T7 and T11 at the bottom. At most of the time, the temperatures at the same height are very close. This verifies the assumption that only temperature gradient exists along the thickness direction.

To exhibit the temperature distribution throughout the slab, the temperatures at different height are plotted in Fig. 4. One can find that the temperature gradient along the thickness direction is non-uniform and non-linear in the day time, when the temperatures vary greatly. Consequently, stresses will be generated in the section even the slab is simply-supported. When temperatures become stable, temperature gradient along the thickness direction is rather linear.

3.2. Thermodynamic analysis

In practice, the temperature field of an entire structure is usually not available. A thermodynamic model is used here to predict the temperature distribution throughout

the structure. Two different thermal boundary conditions will be adopted. The model predictions will be compared with the measurement data.

A 3-D heat conductivity model is established in ANSYS [23] as shown in Fig. 5. There are 6 identical elements in the thickness direction with height of 20 mm each. The mesh is descretized for both thermal analysis and mechanics analysis. Element type SOLID90 is employed for thermal analysis while SOLID65 is employed for mechanics analysis, which will be described later. As we assume that the temperature is uniformly distributed in the horizontal direction, temperature gradient occurs in the thickness direction only.

In the literatures and practical exercises, some measured the structural surface temperatures and some obtained air temperature only. In the present study, these two cases and the corresponding thermal boundary conditions are considered. In the former situation, the top surface temperature $T1$ and bottom surface temperature $T7$ measured at different time are known and regarded as boundary conditions of the slab. Therefore, the temperature of all the nodes at the top is set to $T1$ and the temperature of all the nodes at the bottom is set to $T7$.

In the second case, the air temperature is given. To consider the heat exchange condition between the slab and the surrounding environment, solar irradiation can be measured in-situ or simulated from theoretical models as [24]

$$I = I_d + I_i + I_r \tag{1}$$

where I, I_d, I_i and I_r are the total solar irradiation, direct solar irradiation, diffuse solar irradiation and reflected solar irradiation on a surface, respectively. The model takes into account of the nature of solar irradiation, the geometric relation between the sun and the earth, and the characteristics of the solar energy that reaches the surface of a structure. Then the energy exchange between the surface elements of the slab and the air can be expressed as [24]

$$-k\frac{\partial T}{\partial n} = h(T_s - T_a) - \alpha I \tag{2}$$

where k is thermal conductivity, T is temperature, n is normal to the surface, h is the heat transfer coefficient, T_s is the surface temperature, T_a is the ambient air temperature, α is the absorptivity coefficient of the surface material, and I irradiation. For the bottom elements of the slab, Eq. (2) is similarly applied except that I includes the reflected solar irradiation only. The solar irradiation at the top surface and bottom surface of the slab is then calculated and listed in Table 1. It is noted that in the afternoon, the solar irradiation at the top surface includes the diffuse solar irradiation only because the direct irradiation was blocked.

A transient thermal analysis is conducted to obtain the interior temperature at every time step (2 minutes here). In this analysis, k = 1.74 W/(m·ºC), c = 920 J/(kg·ºC), h = 23 W/(m^2·ºC) for the top surface and 8.7 W/(m^2·ºC) for the bottom surface, and α = 0.7, which are obtained from the Chinese code [25]. Density of the concrete was measured as 2316.3 kg/m^3. Fig. 6 compares the temperatures at different points along the

thickness direction of the slab using both cases of thermal boundary conditions with the measurement counterparts. A very good agreement is found among the three sets of data. This verifies that the numerical model and boundary conditions can be employed to predict the temperature distribution of the slab. For simple structures like the slab employed here, the thermodynamic model is accurate enough. For a practical structure with complicated configuration, the boundary conditions can be more complicated. This can be found in some works done in bridge engineering [26][27].

4. Vibration data

4.1. Modal properties of the slab

Typical measured mode shapes of the first four modes are shown in Fig. 7. Modes 1, 2 and 4 are bending modes and mode 3 is a torsional one. In addition, a set of modal testing was implemented hourly from 8:00 am to 22:00 pm on 11th Feb., 2009 to extract the frequencies and damping ratios.

4.2. Variation of frequency and damping ratio versus temperature change

Fig. 8 illustrates the variation of the measured first natural frequency with respect to the temperatures measured from the thermocouples. It clearly shows that the frequency of the structure decreases when temperature goes up before noon while the frequency

increases as temperature drops down in the afternoon, as observed by many researchers. Variation of the higher modes will be presented later (Fig. 10). However, temperature effect on damping ratios is not so obvious. Fig. 9 illustrates the variation of the first two modal damping ratios extracted from measurement with respect to time. It has been found that damping ratios increase slightly when temperature arise [20]. Since the variation of temperature here is not significant and uncertainty level of measurement of damping is relatively high, the change of damping may be masked by the measurement noise.

The linear regression technique is then utilized to analyze the relation between the frequency and temperature. A multiple linear regression model has the form of [28]

$$f = \beta_0 + \beta_1 t_1 + ... + \beta_p t_p + \varepsilon_f \quad (3)$$

where f is the frequency, β_0 to β_p are the regression coefficients and ε_f is the regression error, $t_1 \sim t_p$ are the temperature explanatory variables. A few cases of temperatures are studied here.

First, the 7 structural temperatures measured ($T1$ to $T7$) are used as the explanatory variables (p=7). With the least-square fitting [28], the regression coefficients are computed. The square of the correlation coefficient R^2 is 0.97 and the standard deviation of the error is 0.03 Hz, which means a very good correlation between the frequency and the temperatures. In literature, some researchers have chosen air temperature, average of the structural surface temperatures (i.e., ($T1$+$T7$)/2), and

differential of the surface temperatures (i.e., ($T1$-$T7$)/2) as explanatory variables. These are also applied to the present experimental data and correspondingly only one temperature variable is used in Eq. (3). The R^2 statistics are calculated as 0.74, 0.88, and 0.18, respectively and the standard deviations of the error are 0.07 Hz, 0.05 Hz, and 0.13 Hz, respectively. This indicates that the structural frequency is not only affected by the air temperature or structural surface temperatures, but also by temperatures at all components of the structure. When one investigates the temperature effect on the vibration properties of a structure, consideration of temperature distribution throughout the structure will improve the correlation.

It is widely accepted that Young's moduli of materials decrease as temperature of the material increases and thus the natural frequencies decrease. When the thermal field of the structure is non-uniform, the structure can be regarded as a composite structure that has different Young's moduli at different components. The natural frequencies can then be calculated. This is demonstrated in the following section.

4.3 Quantification of temperature effect

Although variation of frequencies may be due to many reasons, thermal dependent property of concrete is solely studied here. This is because the slab is simply supported and the physical boundary condition can be regarded as unchanged during the day. In previous study by the first author and his colleagues [20], it has shown that the friction

at the supports and the geometric variation due to temperature change has much less effect on the frequencies, as compared with the variation of Young's modulus with respect to temperature.

Young's modulus of concrete with respect to temperature can be represented as a linear equation, in the range of natural temperature:

$$E(T) = E_{20^\circ C}[1 - \theta_E(T - 20)] \quad (4)$$

where T is the temperature of the material, $E_{20^\circ C}$ is Young's modulus of concrete at the temperature 20℃ and θ_E is the temperature coefficient of Young's modulus, which is suggested as 0.003 by CEP/FIP [29]. This implies that when the temperature of a RC structure goes up by 1℃ uniformly, the natural frequencies drop down by 0.15%. Therefore, when a structure experiences 20℃ change, the natural frequencies may change by 3.0%, which is not small as compared with those due to local damages.

The model in ANSYS shown in Fig. 5 is employed here to calculate the natural frequencies of the slab. At temperature of 20℃, the Young's modulus of each element is 26.0 GPa, which was measured from static tests on three standard cylinder specimens. Poisson's Ratio is set to 0.3 as usual. The first 2 modal frequencies are calculated as 20.30 Hz and 81.25 Hz, quite close to the measurement (19.92 Hz and 82.16 Hz, respectively). The model is not updated here to match the measurement as this is not the objective of the present study.

At different time of the date, the temperature at each element of the slab has been calculated forgoing and the Young's modulus of each element is temperature dependent as described in Eq. (4). These are inputted into the ANSYS model to calculate the frequencies. Variation of the first frequency with respect to time is shown in Fig. 10, as compared with the measurement. As the Young's moduli used in numerical analysis are not exactly the same as the real ones, the frequencies differ from the measurements. To make comparison of the frequency change, the frequencies are normalized with the first values. One can find that there is a good agreement between the numerical results and measurements. This verifies that the variation of structural vibration properties is affected by the structural temperature distribution. Variation of the second and third measured bending frequencies is shown in Fig. 11, as compared with the analytical counterparts. It shows that the variation trend of the measured higher modal frequencies matches that of the analytical one. One can also observe that the discrepancy of the higher modes is larger than the first mode. This may be because the higher modes are not easy to be measured accurately in the case. Moreover, the first torsion mode cannot be reliably identified in some experiments and the results are not shown here. This might be because the supports are not ideally flat and partial of the slab does not contact with the support perfectly, which causes significant error of the measurement.

5. Conclusions and discussions

This paper proposed a new approach to quantify the variation of structural vibration characteristics with respect to structural temperatures. Being different from the conventional studies that using air temperature or temperatures at a few points of the structure, the paper aims to obtain the thermal distribution of the entire structure from the thermodynamic models. Consequently the relation between the frequencies and the temperature at the whole structure is established. The frequencies can also be calculated from the FE model according to the thermal-dependent properties of the material. Both the frequencies and temperature distribution can be compared with the measurement to verify the numerical models.

Application to a simple RC slab has found that the thermodynamic models can predict the structural temperature field accurately. Two different sorts of thermal boundary conditions were applied. In the first condition, the surface temperatures were given, and in the second, only the air temperature was provided and the solar irradiation was numerically simulated. Both gave similar temperature distribution of the slab along the thickness direction. This indicates that in the practice, structural temperature field can be predicted with a few critical temperature data at an acceptable accuracy. For more complicated structures with complex configurations, the first sort of thermal boundary condition requires more temperature measurements, while the second sort of boundary

condition is more convenient. In the heat transfer analysis, many thermal parameters of material obtained from design code or based on experience may affect the analytical results significantly. This causes the accurate prediction more difficult.

Linear regression analysis has discovered that the first natural frequency has a better linear relation with the temperature values at seven different points than with the air temperature and/or surface temperatures only. This verifies that the frequencies are global properties and associated with the temperature distribution of the entire structure. Therefore, consideration of temperature distribution of a whole structure will lead to more accurate results of the temperature effect on the vibration properties of the structure.

Temperature effect on steel bar is not considered in the paper. One reason lies in that temperature coefficient of Young's modulus of steel $\theta_E = 3.6\times10^{-4}/^{\circ}\mathrm{C}$ [30], which is much smaller than that of concrete as 0.003 [29].

ACKNOWLEDGEMENTS

The work performed in this paper is supported by the Hong Kong Polytechnic University Niche Areas Fund (Project No. 1-BB6G) and Shenzhen University Basic Research Grant (Project No. 201045).

REFERENCES

[1] Doebling SW, Farrar CR Prime MB. A summary review of vibration-based damage identification methods. The Shock and Vibration Digest 1998; 30(2):91-105.

[2] Sohn H, Farrar CR, Hemez FM, Shunk DD, Stinemates DW, Nadler BR. A review of structural health monitoring literature: 1996-2001. Los Alamos National Laboratory Report LA-13976-MS. Los Alamos National Laboratory; 2003.

[3] Xia Y, Hao H, Deeks AJ. Dynamic assessment of shear connectors in slab-girder bridges. Engineering Structures 2007; 29 (7): 1475-1486.

[4] Zhou HF, Ni YQ, Ko JM. Constructing input to neural networks for modeling temperature-caused modal variability: Mean temperatures, effective temperatures, and principal components of temperatures, Engineering Structures 2010; 32 (6): 1747-1759.

[5] Salawu OS. Detection of structural damage through changes in frequency: a review. Engineering Structures 1997; 19(9):718-23.

[6] Kim JT, Park, JH, Lee, BJ. Vibration-based damage monitoring in model plate-girder bridges under uncertain temperature conditions. Engineering Structures 2007; 29 (7): 1354-1365.

[7] Askegaard V, Mossing P. Long term observation of RC-bridge using changes in natural frequency. Nordic Concrete Research 1988; 7:20-7.

[8] Cornwell P, Farrar CR, Doebling SW, Sohn H. Environmental variability of modal properties. Experimental Techniques 1999; 23(6):45-8.

[9] Peeters B, De Roeck G. One-year monitoring of the Z24-Bridge: Environmental effects versus damage events. Earthquake Engineering and Structural Dynamics 2001; 30(2):149-71.

[10] Desjardins SL, Londono NA, Lau DT, Khoo H. Real-time data processing, analysis and visualization for structural monitoring of the confederation bridge. Advances in Structural Engineering 2006; 9 (1): 141-157.

[11] Song W. Dyke SJ. Ambient vibration based modal identification of the Emerson bridge considering temperature effects. In: 4th World Conference on Structural Control and Monitoring. 2006 July 11-13, San Diego, USA.

[12] Ni YQ, Hua XG, Fan KQ, Ko JM. Correlating modal properties with temperature using long-term monitoring data and support vector machine technique. Engineering Structures 2005; 27(12):1762-1773.

[13] Ni YQ, Ko JM, Hua XG, Zhou HF. Variability of measured modal frequencies of a cable-stayed bridge under different wind conditions. Smart Structures and Systems 2007; 3 (3): 341-356.

[14] Fu Y, DeWolf JT. Monitoring and Analysis of a Bridge with Partially Restrained Bearings. Journal of Bridge Engineering, ASCE 2001; 6 (1): 23–29.

[15] Liu CY, DeWolf JT. Effect of Temperature on Modal Variability of a Curved Concrete Bridge under Ambient Loads. Journal Structural Engineering, ASCE 2007; 133 (12): 1742-1751.

[16] Breccolotti M, Franceschini G, Materazzi AL. Sensitivity of Dynamic Methods for Damage Detection in Structural Concrete Bridges. Shock and Vibration 2004; 11: 383–394.

[17] Macdonald JHG, Daniell WE. Variation of Modal Parameters of a Cable-stayed Bridge Identified from Ambient Vibration Measurements and FE Modelling. Engineering Structures 2005; 27 (13): 1916-1930.

[18] Nayeri RD, Masri SF, Ghanem RG, Nigbor RL. A Novel Approach for the Structural Identification and Monitoring of a Full-Scale 17-Story Building based on Ambient Vibration Measurements. Smart Materials and Structures 2008; 17 (2): 1-19.

[19] Balmes E, Basseville M, Bourquin F, Mevel L, Nasser H, Treyssede F. Merging Sensor Data from Multiple Temperature Scenarios for Vibration Monitoring of Civil Structures. Structural Health Monitoring 2008; 7 (2): 129-142.

[20] Xia Y, Hao H, Zanardo G, Deeks A. Long term vibration monitoring of an RC slab: Temperature and humidity effect. Engineering Structures 2006; 28 (3):441-52.

[21] National Standards of PRC, Code for design of concrete structures. GB 50010-2002, 2002, in Chinese.

[22] Ewins DJ. Modal Testing – Theory, Practice and Application. Research Studies Press Ltd: Baldock, Hertfordshire, UK; 2000.

[23] ANSYS 8.1. Southpointe (PA, USA): ANSYS Inc.; 2004.

[24] Rohsenow WM. Handbook of heat transfer applications. New York: McGraw-Hill, 1988.

[25] National Standards of PRC, Thermal design code for civil buildings, GB50176-93, 1993, in Chinese

[26] Elbadry MM, Ghali A. Temperature Variations in Concrete Bridges. Journal of Structural Engineering, ASCE 1983; 109 (10): 2355-2374.

[27] Fu HC, Ng SF, Cheung MS. Thermal Behavior of Composite Bridges. Journal Structural Engineering, ASCE 1990; 116 (12): 3302-3323.

[28] Kottegoda NT, Rosso R. Statistics, Probability, and Reliability for Civil and Environmental Engineers. McGraw-Hill Companies, Inc.; 1997.

[29] CEB-FIP. Model Code 1990. London: Thomas Telford; 1993.

[30] Brockenbrough RL, Merritt, FS. Structural Steel Designer's Handbook, 2nd ed., New York, McGraw-Hill; 1994.

Fig. 1a. The RC slab

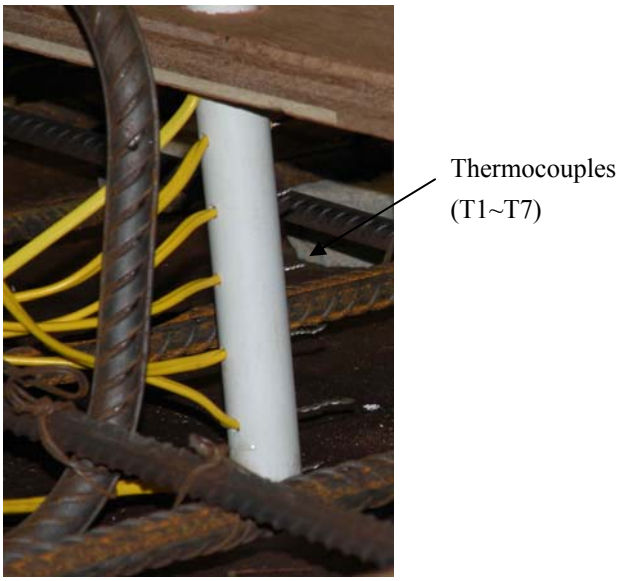

Fig. 1b. Positioning thermocouples inside the slab

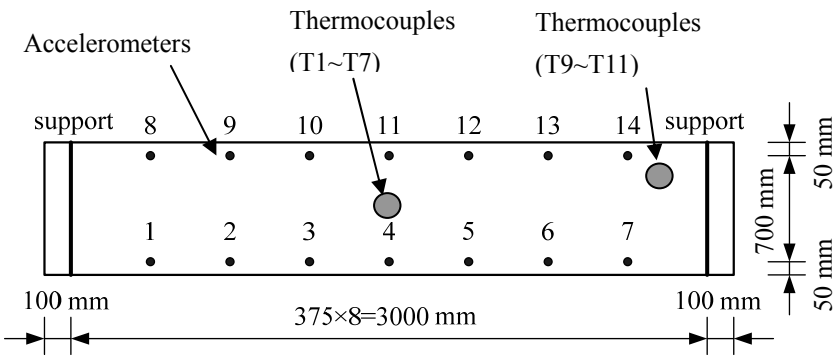

Fig. 1c. Plan position of the sensors

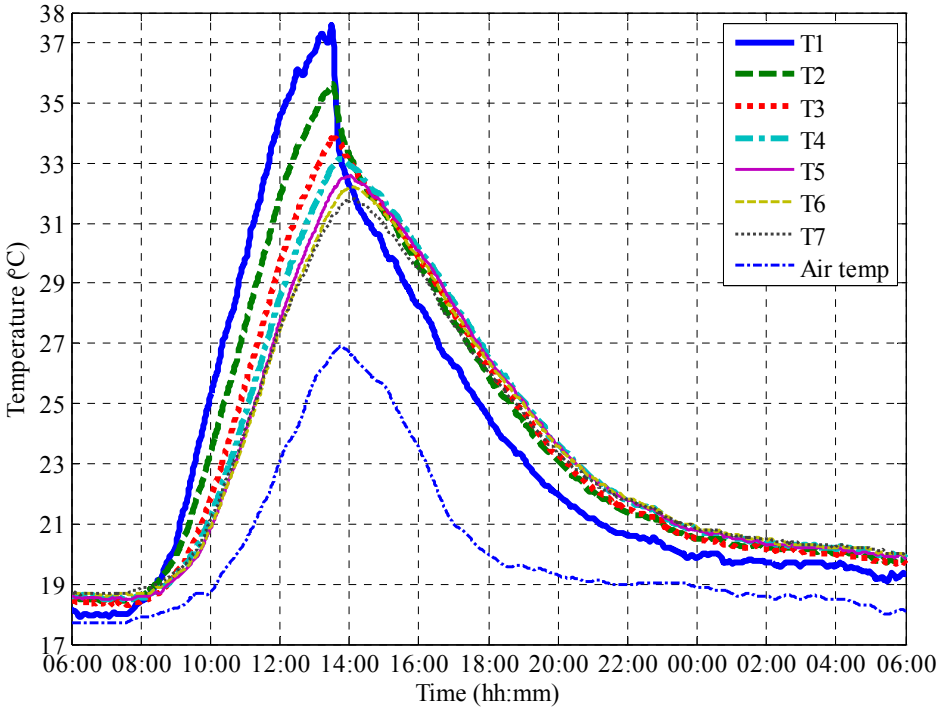

Fig. 2. Variation of the temperatures at the slab in a 24-hour period

(air temp: ambient temperature)

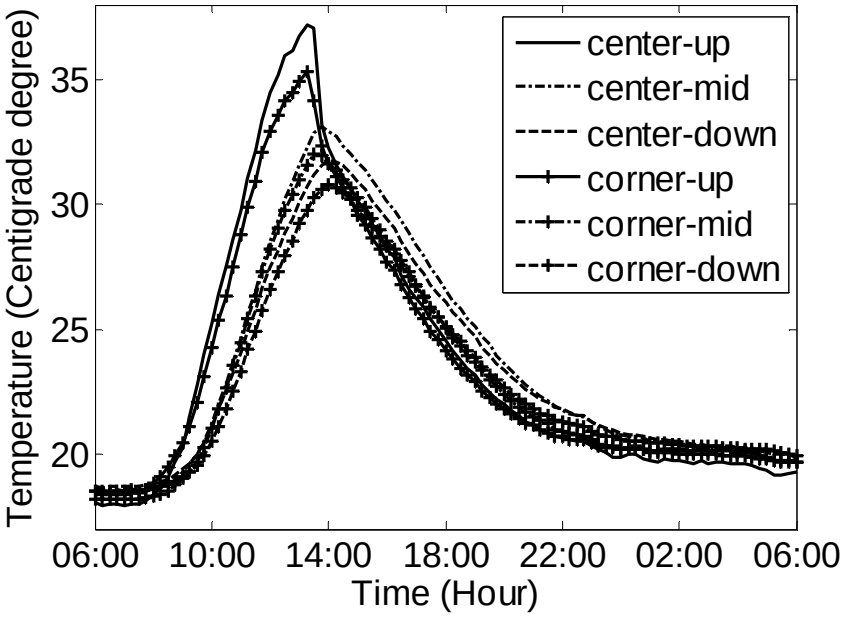

Fig. 3. Comparison between the temperatures at the center and the temperatures at the corner of the slab

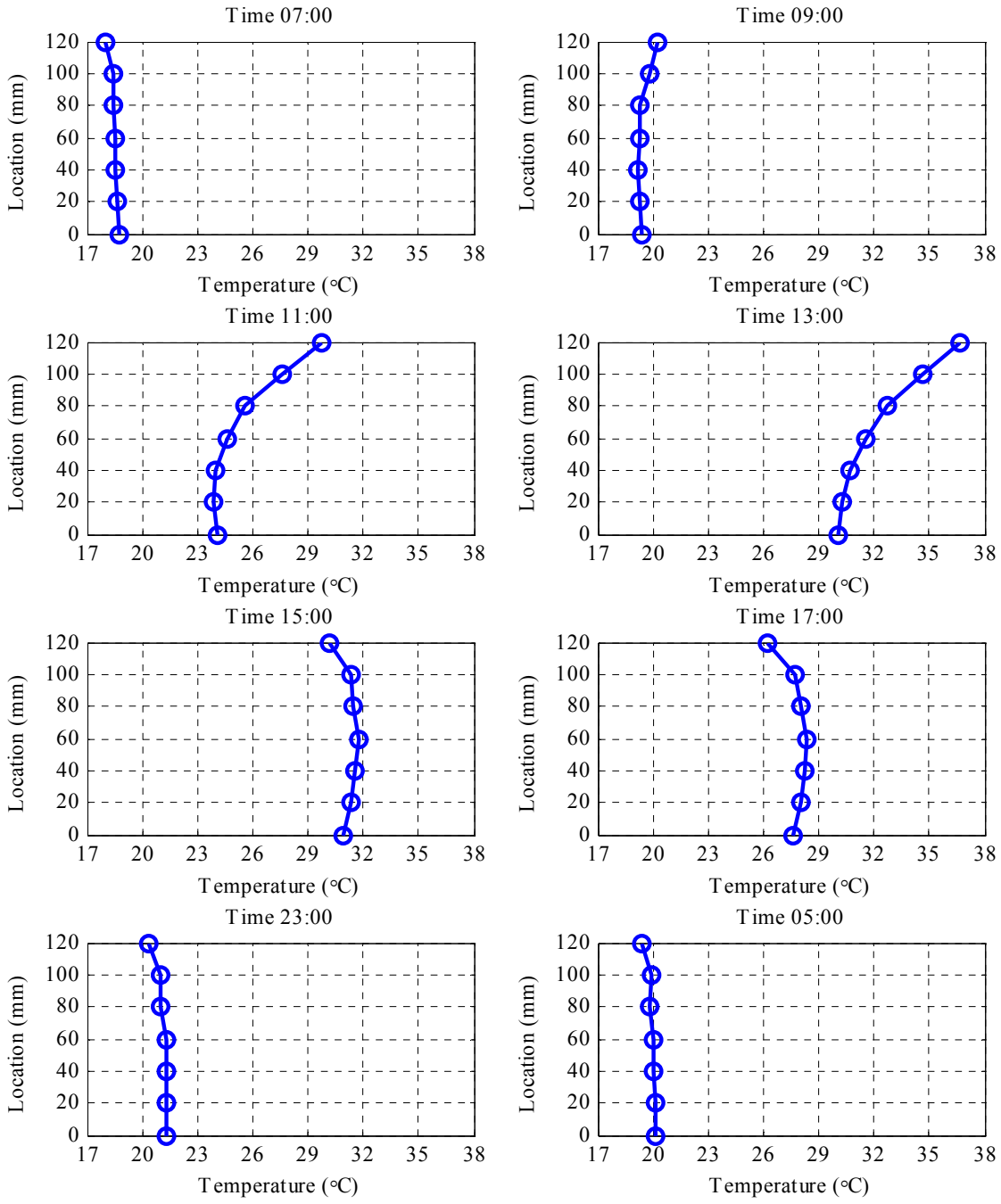

Fig. 4. Temperature distribution along the thickness direction of the slab at different time

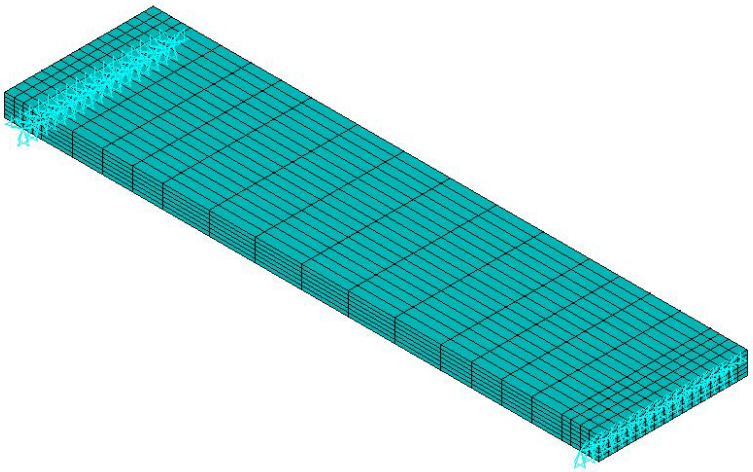

Fig. 5 Finite element model of the slab constructed with ANSYS

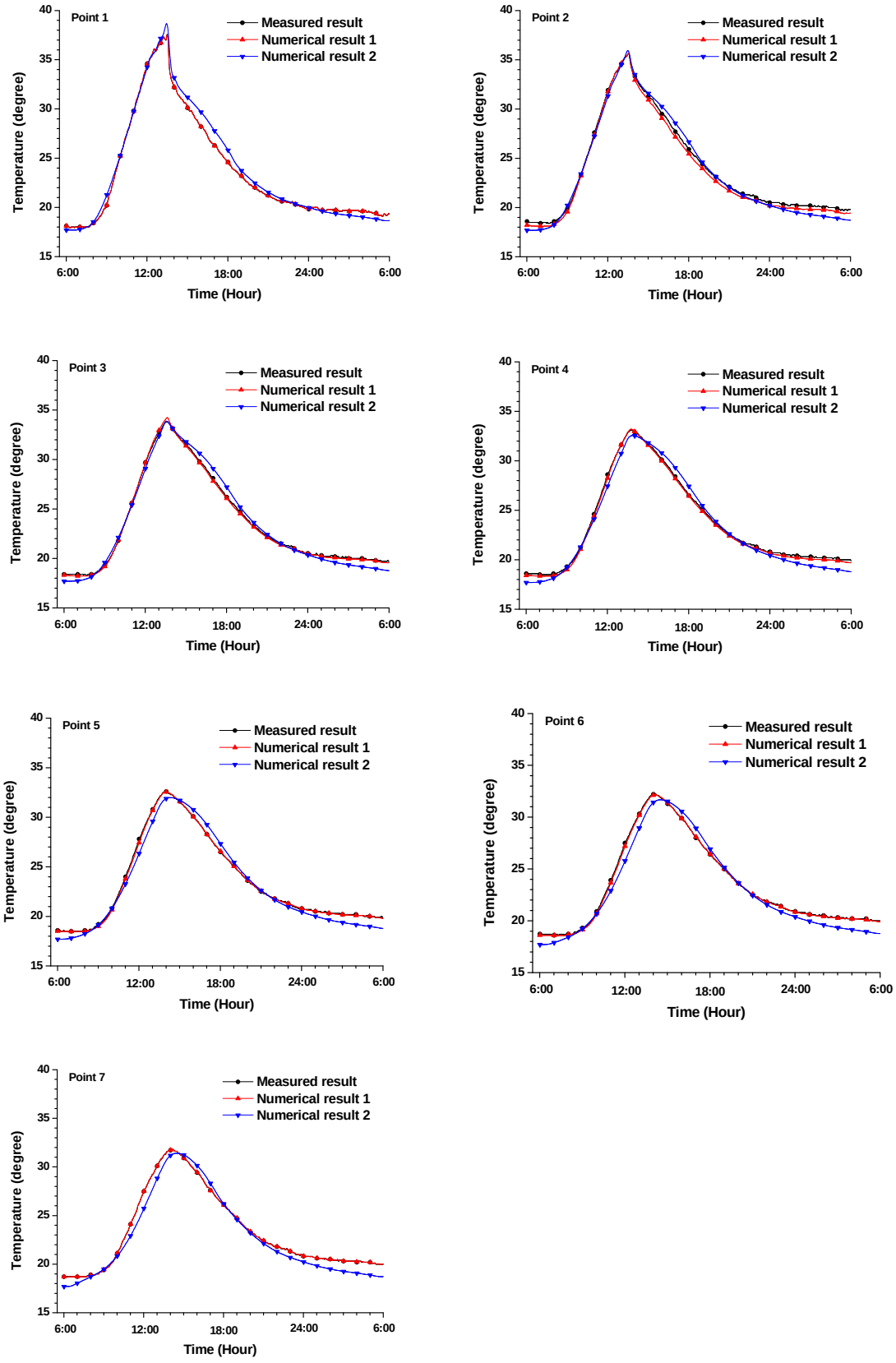

Fig. 6 Comparison of temperature data: model prediction vs. measurement

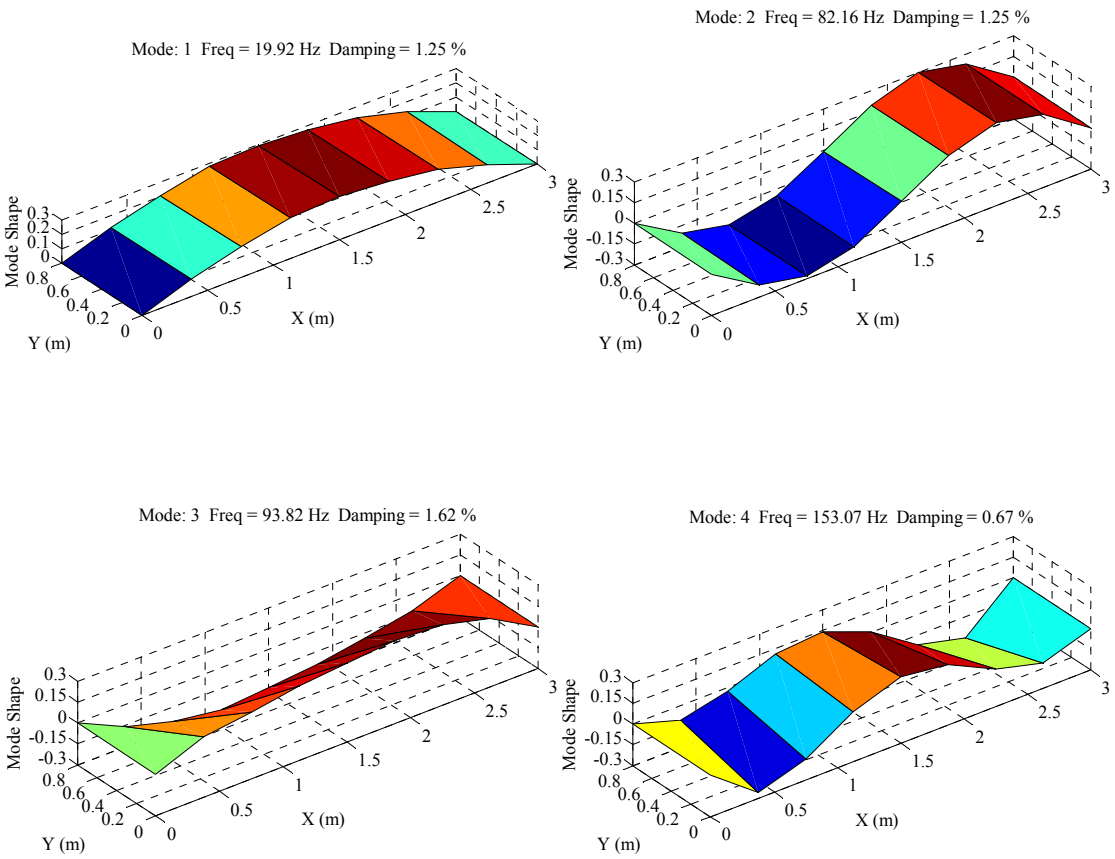

Fig. 7 The measured first four mode shapes of the slab

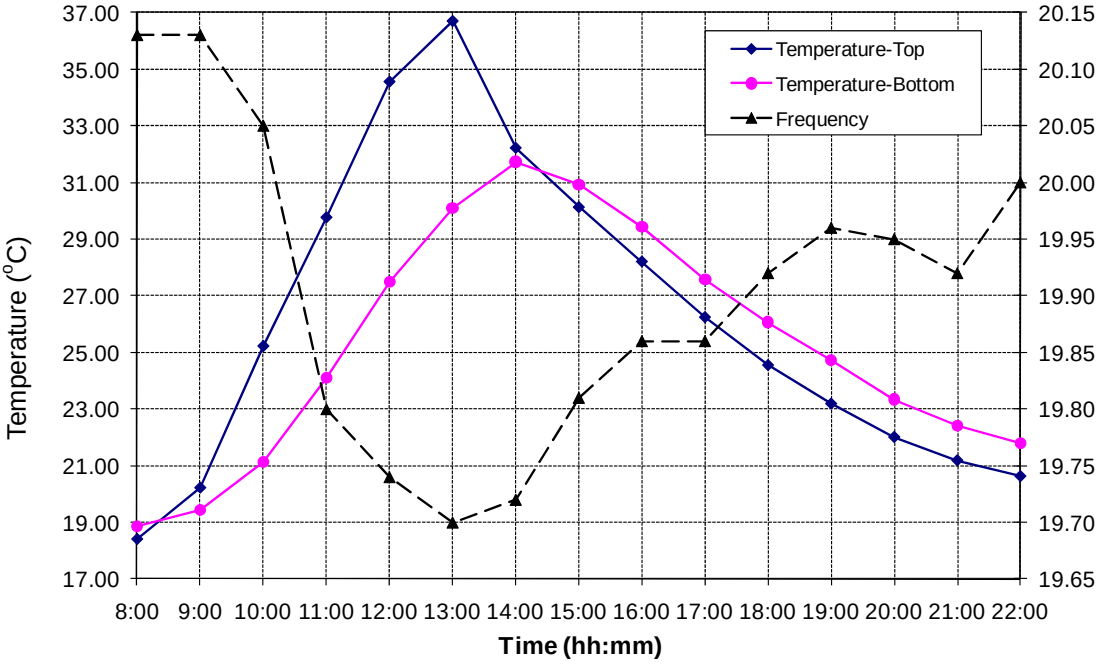

Fig. 8 Variation of the first frequency versus temperatures

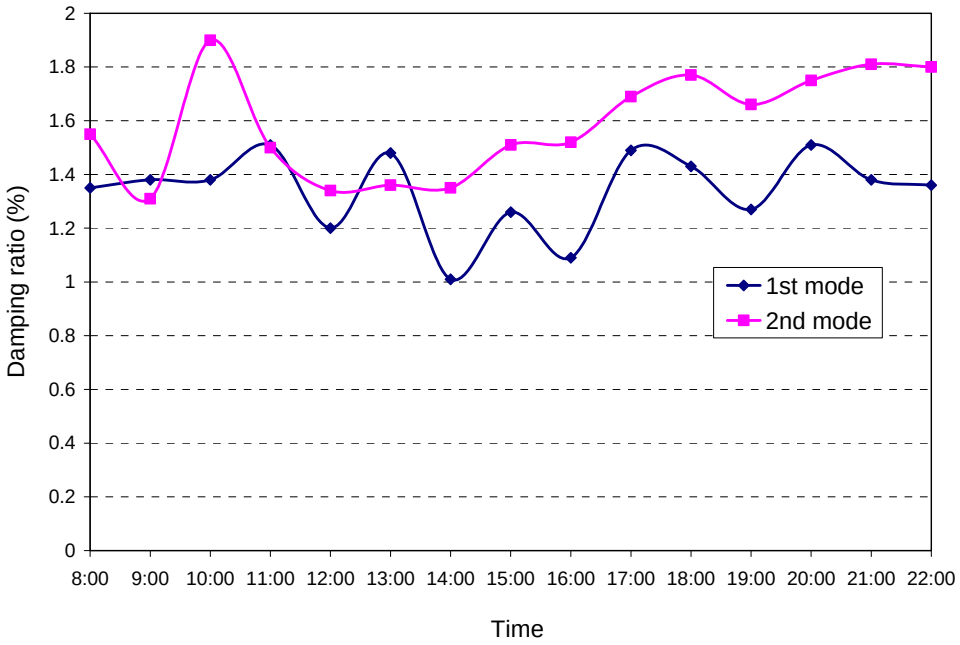

Fig. 9 Variation of the damping ratios

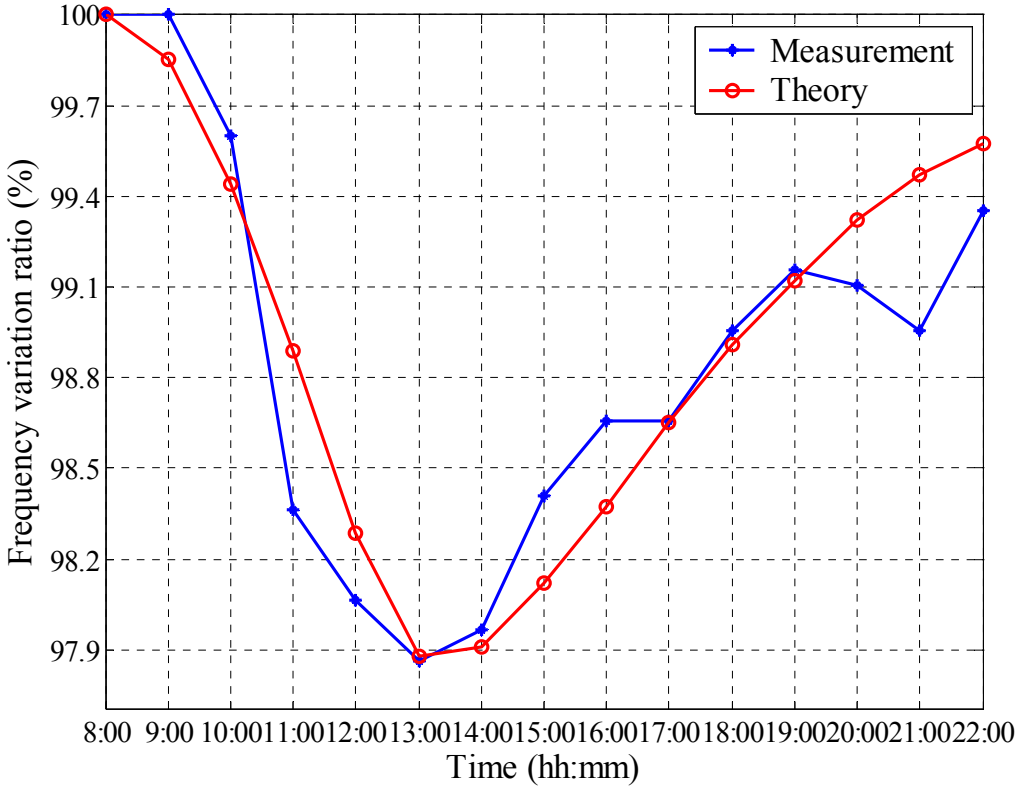

Fig. 10 Comparison of the frequency variation between the measurement and numerical analysis (the 1st bending mode)

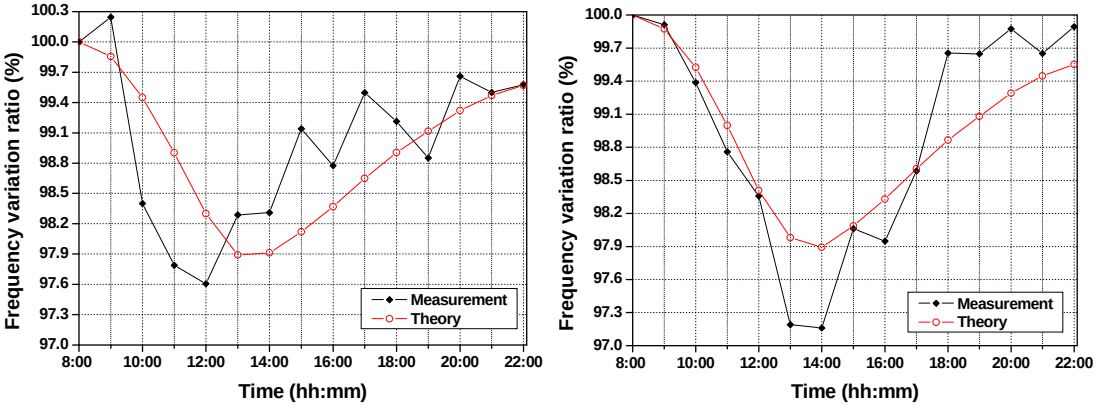

(a) The 2nd bending frequency (b) The 3rd bending frequency

Fig. 11 Comparison of the frequency variation between the measurement and numerical analysis (the 2nd and 3rd bending modes)

Table 1. The solar irradiation on the slab at different time

Time	Solar intensity at top surface (W/m^2)	Solar intensity at bottom surface (W/m^2)
06:00 am	1.0	2.3
07:00 am	6.9	29.0
08:00 am	56.6	52.2
09:00 am	223.8	60.8
10:00 am	403.7	64.8
11:00 am	550.2	66.7
12:00 pm	644.4	67.2
13:00 pm	676.7	66.7
14:00 pm	106.7	64.8
15:00 pm	103.7	60.8
16:00 pm	97.3	52.2
17:00 pm	83.5	29.0
18:00 pm	46.4	1.2